REPORT DOCUMENTATION PAGE

Form Approved
OMB No. 0704-0188

PLEASE DO NOT RETURN YOUR FORM TO THE ABOVE ADDRESS.

1. REPORT DATE *(DD-MM-YYYY)*	2. REPORT TYPE	3. DATES COVERED *(From - To)*
25-09-2013	Performance/Technical Report (Monthly)	8/26/13 - 9/25/13

4. TITLE AND SUBTITLE

Polyfibroblast: A Self-Healing and Galvanic Protection Additive

5a. CONTRACT NUMBER

5b. GRANT NUMBER
N00014-09-1-0383

5c. PROGRAM ELEMENT NUMBER

6. AUTHOR(S)

Benkoski, Jason J.

5d. PROJECT NUMBER

5e. TASK NUMBER
FGY25

5f. WORK UNIT NUMBER

7. PERFORMING ORGANIZATION NAME(S) AND ADDRESS(ES)
The Johns Hopkins University Applied Physics Laboratory
11100 Johns Hopkins Rd
Laurel, MD 20723

8. PERFORMING ORGANIZATION REPORT NUMBER

9. SPONSORING/MONITORING AGENCY NAME(S) AND ADDRESS(ES)
Office of Naval Research
875 North Randolph Street
Arlington, VA 22203-1995

10. SPONSOR/MONITOR'S ACRONYM(S)
ONR

11. SPONSOR/MONITOR'S REPORT NUMBER(S)

12. DISTRIBUTION/AVAILABILITY STATEMENT
Approved for Public Release: Distribution is Unlimited.

13. SUPPLEMENTARY NOTES

14. ABSTRACT

The goal of this project is to develop a primer additive that mimics the self-healing ability of skin by forming a polymer scar across scratches. Designed to work with existing military grade primers, Polyfibroblast consists of microscopic, hollow zinc tubes filled with a moisture-cured polyurethane-urea (MCPU). When scratched, the foaming action of a propellant ejects the resin from the broken tubes and completely fills the crack. No catalysts or curing agents are needed since the polymerization is driven by ambient humidity.

15. SUBJECT TERMS
corrosion protection, self-healing, coatings, polymers

16. SECURITY CLASSIFICATION OF:			17. LIMITATION OF ABSTRACT	18. NUMBER OF PAGES	19a. NAME OF RESPONSIBLE PERSON
a. REPORT	b. ABSTRACT	c. THIS PAGE			Jason J Benkoski
U	U	U	UU	9	19b. TELEPHONE NUMBER *(Include area code)* 240-228-5140

INSTRUCTIONS FOR COMPLETING SF 298

1. REPORT DATE. Full publication date, including day, month, if available. Must cite at least the year and be Year 2000 compliant, e.g. 30-06-1998; xx-06-1998; xx-xx-1998.

2. REPORT TYPE. State the type of report, such as final, technical, interim, memorandum, master's thesis, progress, quarterly, research, special, group study, etc.

3. DATES COVERED. Indicate the time during which the work was performed and the report was written, e.g., Jun 1997 - Jun 1998; 1-10 Jun 1996; May - Nov 1998; Nov 1998.

4. TITLE. Enter title and subtitle with volume number and part number, if applicable. On classified documents, enter the title classification in parentheses.

5a. CONTRACT NUMBER. Enter all contract numbers as they appear in the report, e.g. F33615-86-C-5169.

5b. GRANT NUMBER. Enter all grant numbers as they appear in the report, e.g. AFOSR-82-1234.

5c. PROGRAM ELEMENT NUMBER. Enter all program element numbers as they appear in the report, e.g. 61101A.

5d. PROJECT NUMBER. Enter all project numbers as they appear in the report, e.g. 1F665702D1257; ILIR.

5e. TASK NUMBER. Enter all task numbers as they appear in the report, e.g. 05; RF0330201; T4112.

5f. WORK UNIT NUMBER. Enter all work unit numbers as they appear in the report, e.g. 001; AFAPL30480105.

6. AUTHOR(S). Enter name(s) of person(s) responsible for writing the report, performing the research, or credited with the content of the report. The form of entry is the last name, first name, middle initial, and additional qualifiers separated by commas, e.g. Smith, Richard, J, Jr.

7. PERFORMING ORGANIZATION NAME(S) AND ADDRESS(ES). Self-explanatory.

8. PERFORMING ORGANIZATION REPORT NUMBER. Enter all unique alphanumeric report numbers assigned by the performing organization, e.g. BRL-1234; AFWL-TR-85-4017-Vol-21-PT-2.

9. SPONSORING/MONITORING AGENCY NAME(S) AND ADDRESS(ES). Enter the name and address of the organization(s) financially responsible for and monitoring the work.

10. SPONSOR/MONITOR'S ACRONYM(S). Enter, if available, e.g. BRL, ARDEC, NADC.

11. SPONSOR/MONITOR'S REPORT NUMBER(S). Enter report number as assigned by the sponsoring/ monitoring agency, if available, e.g. BRL-TR-829; -215.

12. DISTRIBUTION/AVAILABILITY STATEMENT. Use agency-mandated availability statements to indicate the public availability or distribution limitations of the report. If additional limitations/ restrictions or special markings are indicated, follow agency authorization procedures, e.g. RD/FRD, PROPIN, ITAR, etc. Include copyright information.

13. SUPPLEMENTARY NOTES. Enter information not included elsewhere such as: prepared in cooperation with; translation of; report supersedes; old edition number, etc.

14. ABSTRACT. A brief (approximately 200 words) factual summary of the most significant information.

15. SUBJECT TERMS. Key words or phrases identifying major concepts in the report.

16. SECURITY CLASSIFICATION. Enter security classification in accordance with security classification regulations, e.g. U, C, S, etc. If this form contains classified information, stamp classification level on the top and bottom of this page.

17. LIMITATION OF ABSTRACT. This block must be completed to assign a distribution limitation to the abstract. Enter UU (Unclassified Unlimited) or SAR (Same as Report). An entry in this block is necessary if the abstract is to be limited.

REDD-2013-363

POLYFIBROBLAST: A SELF-HEALING AND GALVANIC PROTECTION ADDITIVE

Progress Report #4

Prepared for:

Frank Furman
Logistics S&T Thrust Manager
Office of Naval Research
Code 30, Room 1149
875 North Randolph Street
Arlington, VA 22203-1995

Prepared by:

Jason J. Benkoski, Ph.D., Senior Research Scientist
The Johns Hopkins University Applied Physics Laboratory
The Milton S. Eisenhower Research Center
11100 Johns Hopkins Rd, MS 21-N109
Laurel, MD 20723
Tel. (240) 228-5140

Reporting Period: August 26, 2013 through September 25
Date of Report: September 25, 2013

TABLE OF CONTENTS

1 Summary

The initial results suggest that dielectric spectroscopy is an effective technique for nondestructive evaluation of microcapsule health within painted coatings. The real and imaginary parts of the dielectric constant appear to increase with microcapsule loading, but they eventually decrease at high loading most likely because of voids. In addition, the corrosion potential (E_{cor}) measured under open-circuit conditions, and electrochemical impedance spectroscopy demonstrate the corrosion-protection role of zinc and silane when a scratch occurs on the painted steel surface.

2 Project Goals and Objectives

The four milestones for phase IV are given below. For the purposes of tracking our progress, we are currently at the end of month 4 in our revised research plan. Most progress this month has focused on the second milestone.

1. Develop on site inspection method for monitoring self-healing and coating health by month 3. (**Completed**)
2. Develop a method for continuous monitoring of OTS degradation by month 5.
3. Demonstrate a method for measuring the fraction of broken microcapsules as a function of shear stress by month 6. (**Completed**)
4. Establish baseline metrics for qualifying batches of microcapsules from the manufacturing process by month 12.

3 Key Accomplishments

3.1 In Situ Microcapsule Health Monitoring

Dielectric spectroscopy measures the complex dielectric constant (ε) as a function of the frequency of an alternating electric field. The complex dielectric constant has a real (ε') and imaginary component (ε''). ε' corresponds to the decrease in electric field within the material relative to the applied electric field. It is usually higher for more polar or polarizable materials. The imaginary component of the dielectric constant relates to the energy dissipated per period of an alternating electric field (W): $W = 2\pi f E \varepsilon''$, where f is the frequency and E is the electric field.

We are attempting to exploit dielectric spectroscopy to monitor the quantity of liquid within the paint. The dielectric constant of the liquid active ingredient, OTS, is about 2.1. If the inclusion of 5-10% (v/v) OTS in the zinc-rich primer changes the dielectric constant, then changes in the dielectric constant may correspond to changes in the quantity of liquid. This nondestructive test therefore has the potential to allow continuous monitoring to the health of the microcapsules while in service. In contrast, Fourier transform infrared spectroscopy, gas chromatography, and thermogravimetric analysis (the current methods) destroy the sample during analysis. These methods also require powdered or dissolved material. They are designed for microcapsule analysis rather than dry paint analysis.

The experiments were performed as follows: First, a printed circuit board was prepared with a set of copper electrodes. Upon the electrodes was applied a self-healing paint with varying amounts of microcapsules (0, 5, 10, and 25% microcapsules per volume of filler). Some samples were used with primer only, while others were prepared with the full CARC stack that include an additional layer of CARC primer and CARC topcoat over the top of the self-healing paint. The electric field was then varied from 200 MHz to 1 GHz. The samples are depicted schematically in Figure 1.

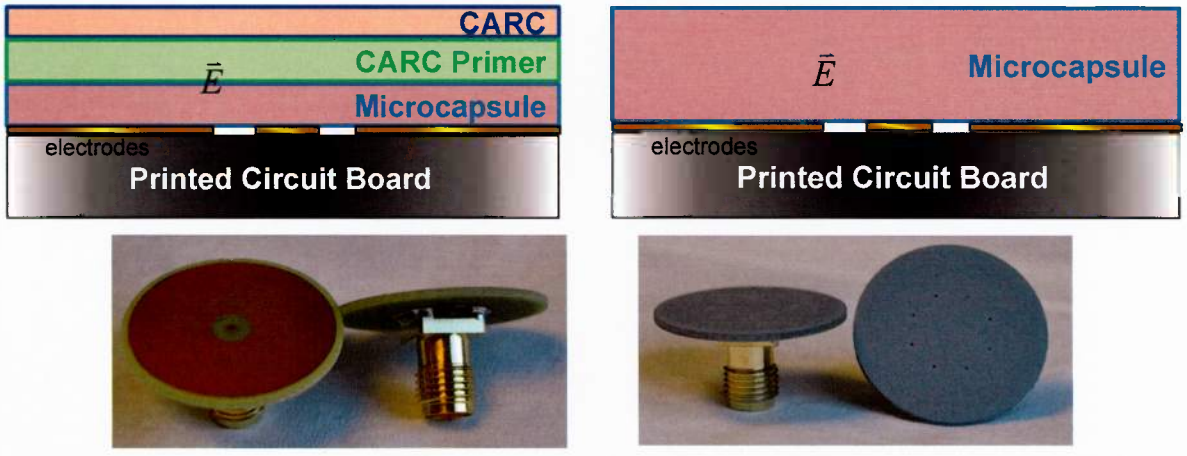

Figure 1: (top row) Schematic representation of dielectric spectroscopy samples. Alternating electrode strips on the printed circuit board apply an alternating electric field that passes through the coating. The measured complex dielectric constant depends on the amount of entrained OTS. Bottom row shows the bare electrode and painted electrode, respectively.

Figure 2 shows the measurements for ε', ε'', $\tan\delta$ (equal to $\varepsilon''/\varepsilon'$), and ε' at 1 GHz divided by ε' at 200 MHz. When plotted versus microcapsule loading, one can see a definite difference in both ε' and ε''. Both appear to increase in going from 0 to 10% (v/v solids), but decrease at 25% relative to the control. The increase at low microcapsule loading presumably results from the OTS-filled microcapsules, but the decrease at 25% microcapsules is harder to interpret. The most likely explanation at this point is that the additional filler causes voids in the dry paint. Zinc-rich paint is formulated to have as much zinc as possible to ensure particle percolation and electrical conductivity. The polymer binder is effectively saturated with solid filler. Any additional filler–dry microcapsules in this case–will most likely make it impossible for the polymer binder to fill all of the space between the zinc particles and microcapsules. These voids will have a dielectric constant of 1, and consequently they will reduce the measured dielectric constant of the paint.

Future experiments will investigate whether it is necessary to also supply additional polymer binder when the microcapsules are mixed into the MIL-P-26915 primer. Specifically, we will look at whether the dielectric constant increases for the 25% microcapsule sample due to the additional binder. If voids in the film are currently causing ε' to decrease, then we would expect ε' to be higher when additional polymer binder is added.

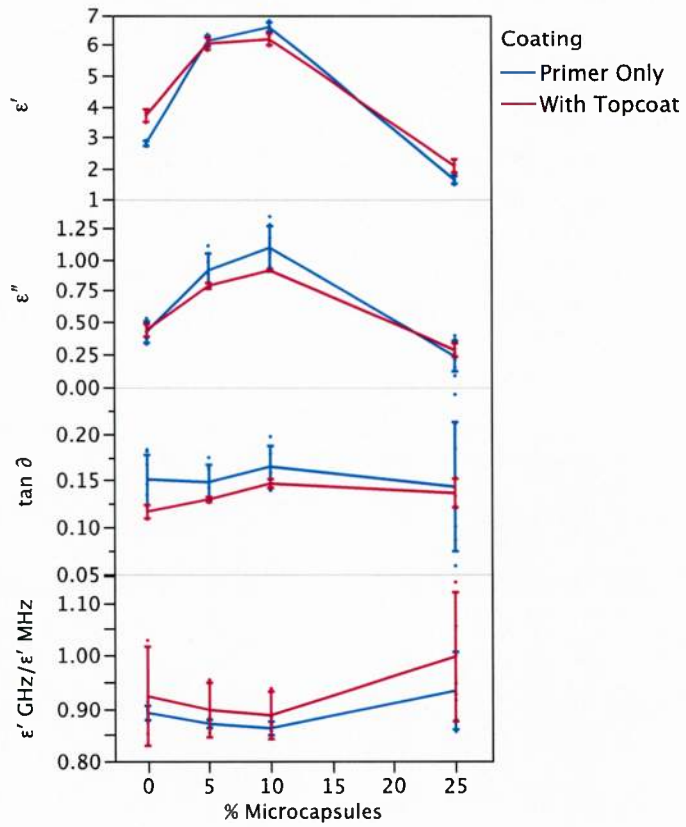

Figure 2: Plot of complex dielectric constant versus microcapsule loading. Both the real and imaginary parts of the dielectric constant showed strong dependence on the microcapsule loading, indicating that this may be a useful method for nondestructive monitoring of the health of the microcapsules within a coating. Neither $\tan\delta$ nor the frequency dependence of the dielectric constant gave a large enough change to be useful for monitoring.

3.2 Direct Measurement of Self-Healing

As described previously, the repair of scratches through the flow of OTS and subsequent formation of a self-assembled monolayer has been measured directly through electrochemical impedance spectroscopy (EIS). EIS works by measuring the complex impedance of a coating that is applied to a metal substrate while immersed in an electrolyte. The resistive, capacitive, and inductive components of the adhesive provide insight into the overall quality of the coating. With respect to self-healing, the recovery of the impedance is a direct measure of the ability of the OTS to protect the underlying steel through passivation.

An example of impedance recovery through self-healing is given in Figure 3. This particular sample shows an initial corrosion resistance of roughly 100 MΩ. The resistance drops to about 0.001 MΩ at the instant that the fresh scratch is made. Then, over the course of 48 hours, the corrosion resistance returns to about 1 MQ. Although the recovered resistance is still 2 orders of magnitude smaller than the original coating, it is still impressive. The 2 nm thick coating of a densely packed molecule has 1% of the corrosion resistance of a three-layer CARC coating that is 70,000x thicker.

This recovery can be described in terms of how it might potentially extend the lifetime of the galvanically protective zinc powder. The corrosion resistance of the bare scratch is three orders of magnitude lower than the healed scratch. Depending on the kinetics of corrosion, this barrier layer may greatly extend the lifetime of galvanic protection supplied by the zinc-rich primer.

Self-healing has been demonstrated by this technique for some time. In the current study, we set out to investigate the effects of microcapsule formulation on the ability to self-heal. Specifically we looked at emulsifier (Gum Arabic vs. SiO_2), polymer-forming monomer (IPDI vs. BCI), silane molecular weight (C12 vs. C18 vs. C8-C18), and electrolyte pH (ASTM G42 pH 7, acetate pH 4.7).

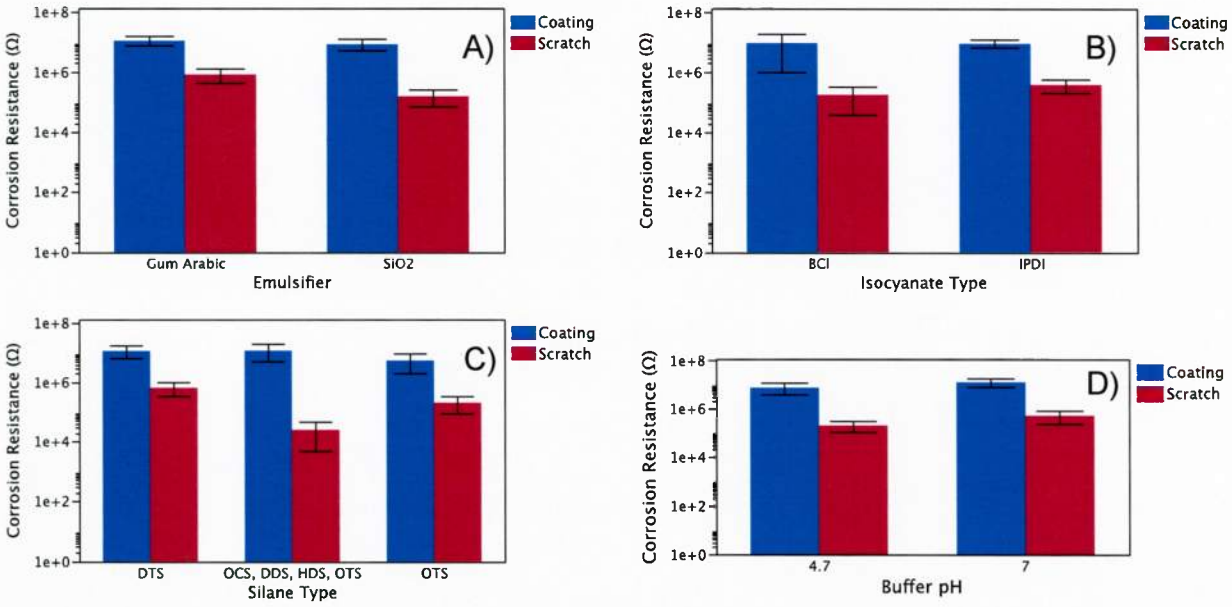

Figure 3: A) Corrosion resistance of the intact coating and scratched coating as a function of A) emulsifier, B) polymer shell-forming monomer, C) silane type, and D) buffer pH.

Due to the small sample size (N = 2 or 4), the results are not as easy to interpret as rust score data. EIS is sensitive to the coating quality, scratch length, and manner of scratching in ways that the simpler rust score is not. We can, however, make a few observations. The effect of the silica nanopowder is not significant on the extent of healing in this measurement. The magnitude of recovery for the Gum Arabic samples was higher, but the % recovery was higher for the silica-enhanced microcapsules. Silica primarily affects shelf life and mechanical durability, so this result is not surprising.

The type of monomer also did not appear to matter in these measurements. Whether polymerized from IPDI or BCI, the extent of self-healing appeared to be roughly the same. Again, the effect of IPDI is to generally improve shelf life relative to BCI. For fresh samples, the self-healing should not vary much.

For silane type, both DTS (12 carbons) and OTS (18 carbons) performed similarly. However, the blend of silanes (8, 12, 16, and 18 carbons) underperformed. Since OTS and DTS act as barrier coatings partly through the ability of the identical molecules to crystallize in 2-dimensions, it is possible that a mixture of silanes will form a disorganized monolayer with many defects.

Lastly, the effects of pH were minor. The corrosion resistance at long times did not vary much, but some samples showed a faster rate of healing in the more acidic buffer. Such a finding is not surprising in light of the fact that OTS hydrolysis is catalyzed by acid. Once activated, the OTS can more effectively form hydrogen bonds and Si-O-Fe bonds with the native oxide of steel.

3.3 Mechanism of Corrosion Protection by Polyfibroblast

The model that we have used to describe the three major steps leading to corrosion protection action by the silane in the Polyfibroblast microcapsules:

1. When a scratch occurs the bare steel surface is exposed to moisture, oxygen and other corrosive agents in the surrounding. However, the zinc in the primer acts as a sacrificial anode and protects the steel from corrosion. The protection by zinc against of steel will last until most of the zinc is consumed.
2. During the course of scratching, microcapsules break, releasing silane on to the steel surface, and the silane molecules adsorb on the bare steel surface. The kinetics of adsorption of long-chain silane on metal surfaces can be slow, hence only a few molecules of silane are adsorbed on the surface immediately following the scratch.
3. As time progresses, more silane molecules adsorbed, creating a barrier layer against water molecules accessing the steel surface.

Two electrochemical techniques that we used to characterize (EIS and E_{cor}) the surface following scratching support the three-step mechanism described above. In all these measurements, the test coupons surfaces were in contact with an aqueous solution of 1%wt. each of sodium carbonate, sulfate and chloride (also used in the ASTM-G42 standard). Figure 4 shows the changes in the corrosion resistance, R_p (measured using EIS) of a coated steel panel that was freshly scratched (scratch dimensions: 1/16-in. wide, ½-in. long). In this case, the coating contained (OTS+IPDI)-filled microcapsule. Soon after the surface scratched, R_p was

relatively small, about 2,000 ohms. However, over the next three days, the R_p increased nearly exponentially to 30,000 ohms, thus offering protection against corrosion. The increase in R_p with exposure time is caused by the barrier layer formed by the slowly adsorbing silane. During the formation of the layer, the steel surface can be vulnerable to corrosion attack, and it is the sacrificial action by zinc that protects the steel from corrosion. Open circuit potential measurements helped established the protection made available by zinc.

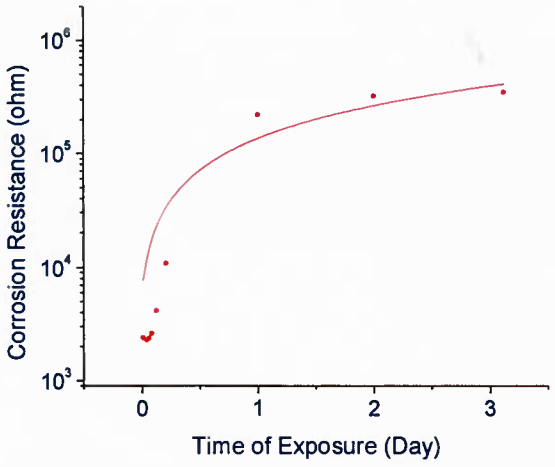

Figure 4: The increasing resistance to corrosion is caused by the slow and continuous adsorption of OTS on to the bare metal surface exposed by the scratch. The data was collected by EIS.

Monitoring open circuit potential, E_{cor} following scratching also helped established the three-step process of corrosion protection by the silane released by breaking microcapsule. This is elucidated by E_{cor} measurements made on three steel coupons with three different types of coatings: 1. Primer only; 2. Zinc-rich primer; 3. Zinc-rich primer with microcapsules. Figure 5 shows E_{cor} data for the first two of the three coupons (Primer only and Zn-rich primer) measured following a surface scratch. Note that the primer-only coupon exhibited a nearly-constant E_{cor} of about -0.55 V (vs. Ag/AgCl/1M KCl reference); most importantly, the value hardly changed with time, as is the behavior of steel in contact with aqueous salt solutions of near-neutral pH. The same figure also shows the E_{cor} behavior for the coupon with a coating containing zinc-rich primer. Soon after the scratch, the E_{cor} registered a large negative value of -1.2 V, typical of cathodic protection of steel by zinc. However, as the zinc was consumed sacrificially, E_{cor} value became positive rising up to -0.8 V.

The last 14 hours of data were collected at close interval of 1 data point per 100 seconds elucidated an important aspect of the E_{cor} behavior and how the zinc works to protect the bare surface of steel. When observed in close intervals of exposure time, E_{cor} showed a noise-like behavior that was intense in the zinc-rich case, fluctuating between -0.8 and -1.1 V. Obviously, E_{cor} can reverse toward -1.1 V only if new zinc becoming available to polarize the potential of steel. Such a possibility does exist, if we assumed loose zinc particulates in the paint near the scratch migrates away from the paint on to the bare steel surface. However, once the new arrival is also consumed sacrificially, the potential of steel goes back to -0.8 V.

The steel coupon with zinc and microcapsule, when scratched, showed a behavior that was different from the first two coupons. The E_{cor} data in Figure 6 demonstrates the crucial aspect of

corrosion protection by steel during the initial period following the scratch; within the first 30 hours after the scratch, E_{cor} moved from -1.2 V to -0.7 V, just as in the case of the zinc-rich primer (no microcapsule). However, the silane released by the breaking microcapsule began to populate the surface, forming a strong barrier to water over the next several hundreds of hours of exposure to the aqueous solution. When the barrier formed, as evidenced by the increasing corrosion resistance, R_p with exposure time (Figure 4), the E_{cor} did not behave the same way as the metal/electrolyte interface behaved in the steel coupons' data shown in Figure 5. A polymer- or silane-coated metal is not governed by the same Nernst relationship as a bare metal/electrolyte interface. In the example shown in Figure 6, E_{cor} reached a large positive value, fluctuating between -0.1 V and 0.06 V, much different from a bare steel surface (-0.55 V) or zinc-coated steel surface (-1.2V). The important aspect of this observation are: i) in presence of the microcapsule in the coating, the scratched surface gets a protective coating by the silane; and ii) zinc does play a critical role of protecting the steel from corroding, until the silane-rich barrier layer is formed over several tens of hours that finally seals almost completely over the next several hundred hours

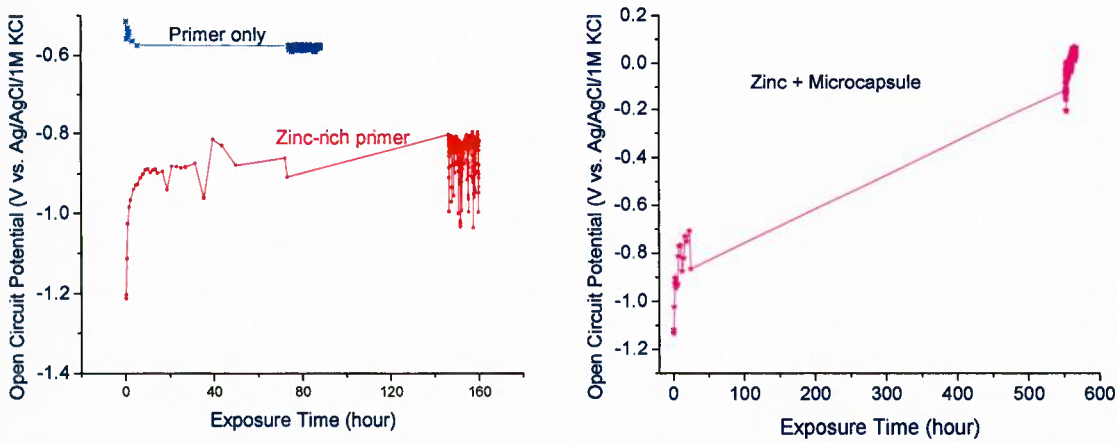

Figure 5: (left): E_{cor} variation following scratching the coating (at Exposure Time = 0 hour), showing a large negative value in the zinc-rich primer only. Even after 180 hours, there is sufficient amount of zinc in the vicinity of the scratch, protecting the bare steel surface from corrosion. This type of prolonged protection is necessary to allow the slow-adsorbing silane to form a protective layer and provide long-term (thousands of hours) of protection against corrosion. (right): E_{cor} variation following scratching the coating (at Exposure Time = 0 hour), showing a large negative value in the zinc-rich primer with microcapsule only. Note that after hundreds of hours, E_{cor} shifts positive to 0.06 V, mainly due to a strong barrier layer formed by silane preventing water from accessing the bare steel surface.

3.4 Next Steps

We will run additional dielectric spectroscopy measurements to ensure the reproducibility of the findings presented in this report. We will also run additional positive and negative controls to verify the hypothesis that the increase in dielectric constant results from the OTS entrained within the coating. Finally, we will mix additional primer into the MIL-P-26915 when the

microcapsules are added to test whether voids are causing the decrease in dielectric constant at high loading.

The electrochemical impedance spectroscopy study is nearly complete. We will primarily be analyzing the data we currently have to extract all useful information before moving forward with additional experiments.